

Lagrangian large-eddy and single-column model simulations of marine cold air outbreaks observed during ACTIVATE



Florian Tornow^{1,2}, Andrew Ackerman², Ann Fridlind², Brian Cairns², Simon Kirschler^{3,4}, Richard Moore⁵, Kenneth Thornhill⁵, George Tselioudis², Christiane Voigt^{3,4}, Luke Ziemba⁵, Armin Sorooshian^{6,7}

¹Center for Climate Systems Research, Columbia University, ²NASA GISS, ³Deutsches Zentrum für Luft- und Raumfahrt (DLR), Oberpfaffenhofen, Germany, ⁴Johannes Gutenberg-Universität, Mainz, Germany, ⁵NASA Langley Research Center, Hampton, VA 23681, USA, ⁶Department of Chemical and Environmental Engineering, University of Arizona, Tucson, Arizona, 85721, USA, ⁷Department of Hydrology and Atmospheric Sciences, University of Arizona, Tucson, Arizona, 85721, USA



1. INTRODUCTION

- ▶ Marine cold air outbreaks (CAOs) appear in mid- and high-latitudes and form low-level clouds that distinctly enhance the local albedo (e.g., Fig. 1)
- ▶ The CAO weather state is deficient in Earth system models (ESMs)^[1] and a bottom-up roadmap aims to improve CAO representation in ESMs:
 - In-situ and remote sensing observations of planetary boundary layer (PBL) and free troposphere (FT) collected during the multi-year NASA EVS-3 campaign ACTIVATE^[2]
 - Understanding factors controlling the observed case and its evolution using large-eddy simulation (LES), focused on microphysics and cloud breakup
 - Evaluation of LES as well as ESM column physics

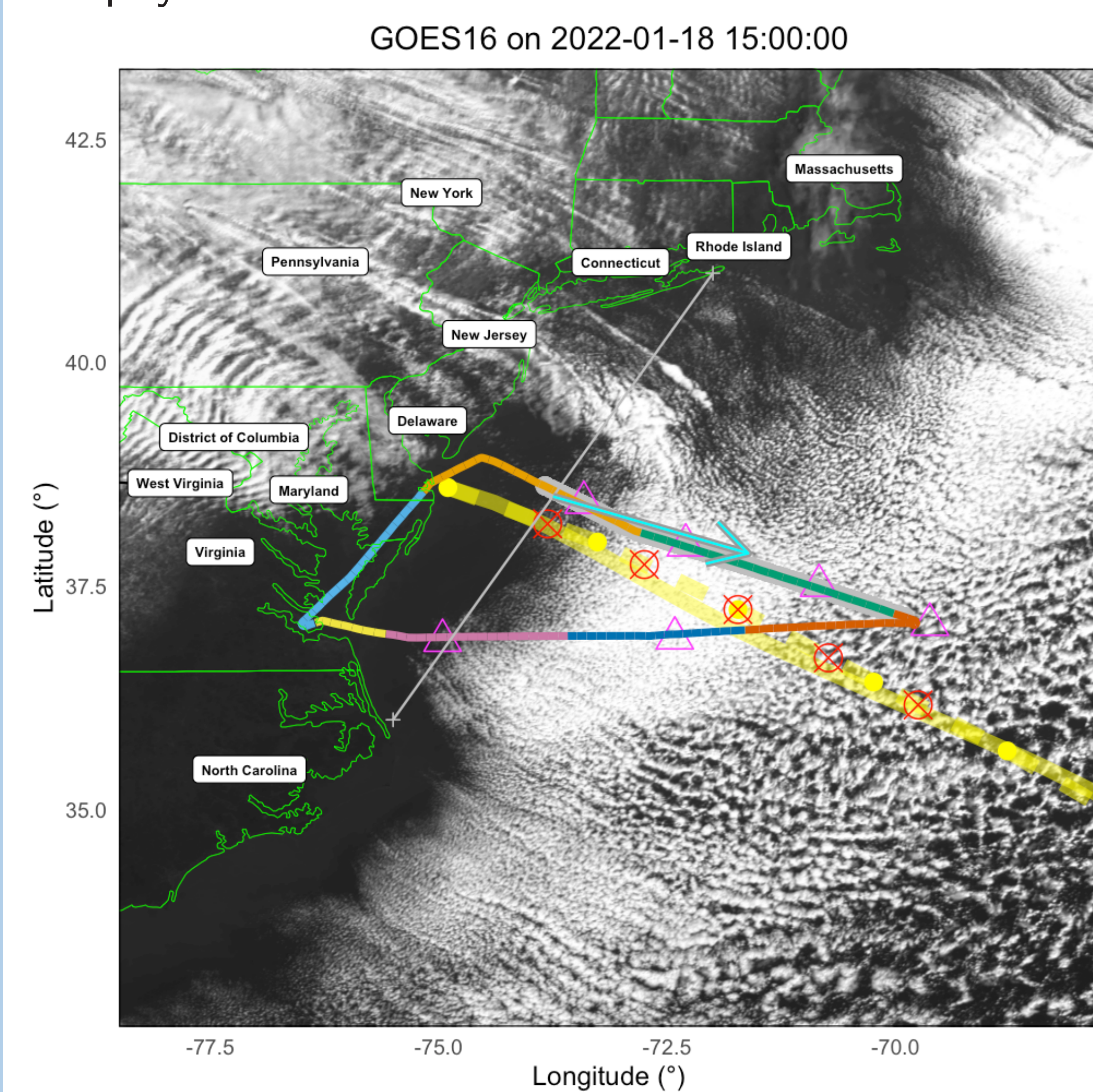


Fig. 1: Exemplary CAO case from 18 January 2022: Flight track (multi-color) with dropsondes (triangles), Lagrangian trajectory (yellow) and simulated 3D domains (X marks with circles). Cloud edge (thin gray) and approximate cloud roll orientation (cyan arrow) allow translation to a quasi-Lagrangian framework.

2. INITIAL AND BOUNDARY CONDITIONS

- ▶ Meteorological fields from MERRA-2 and ERA5 are extracted along Lagrangian trajectories
- ▶ Aerosol number concentrations for PBL and FT are inferred per flight from legs in respective layer that are farthest upwind (where entrainment and cloud interaction has presumably not acted yet^[3]) and earliest in the day (shown in Fig. 2 and listed in Table 2 for 18 Jan. 2022)
- ▶ Hygroscopicity per mode is assumed where CCN measurements are unavailable or not yet processed (such as this exemplary 2022 case)
- ▶ Several cases processed (Table 1); 18 January 2022 characterized by a relatively swift cloud transition

Tab. 1: CAO cases

#	Date
1	1 March 2020
2	3 February 2021
3	11 January 2022
4	18 January 2022
5	13 March 2022
6	29 March 2022

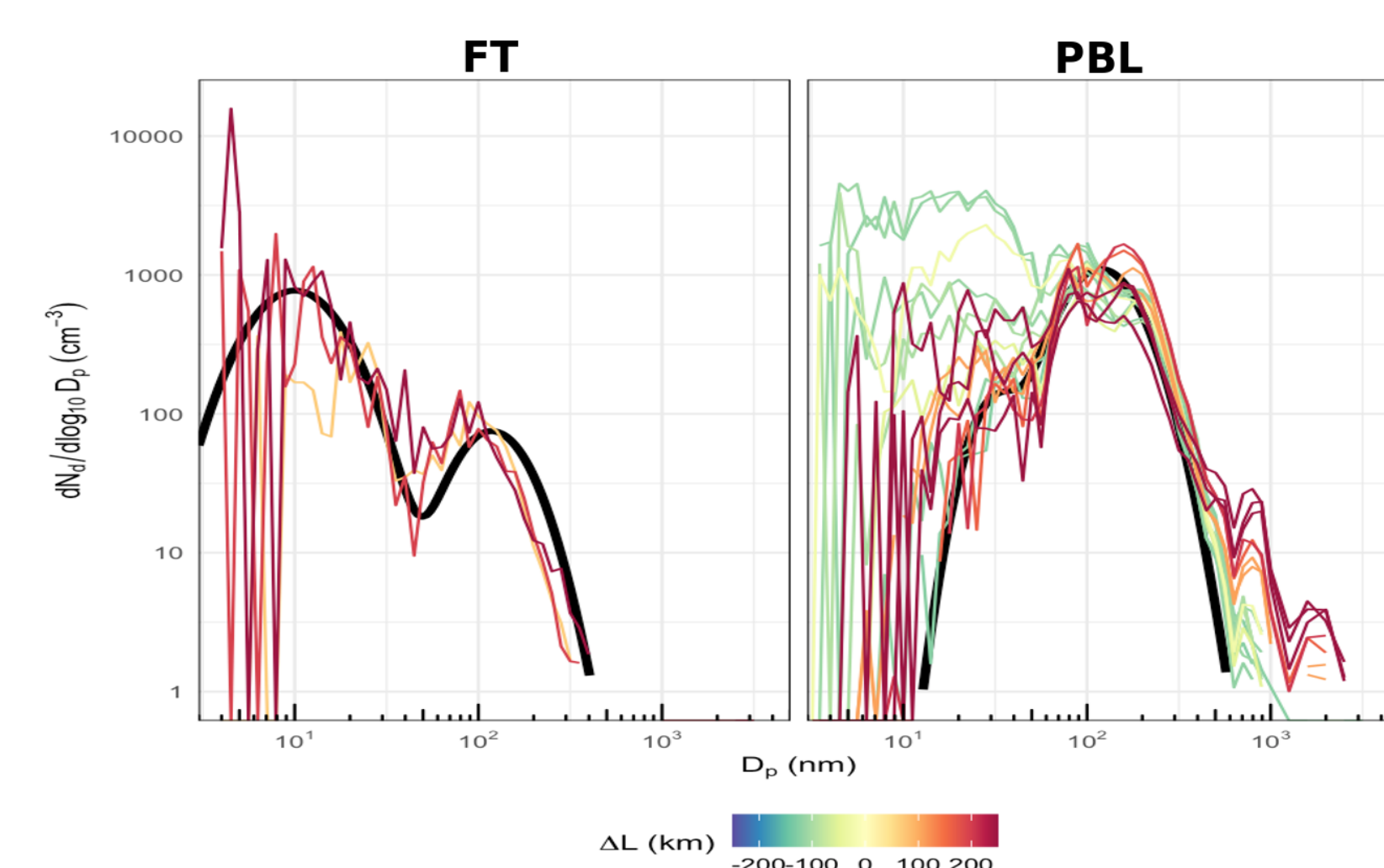


Fig. 2: In-situ measurements of aerosol size distributions are used to initialize simulations (black line); shown per PBL and FT (panels) and by downwind distance (color). Note the elevated concentrations of smaller particles probed on return legs, likely resulting from near-coastal new particle formation^[4].

KEY POINTS

- ▶ ACTIVATE enables better understanding of cloud regime transitions that ESMs struggle with
- ▶ Guided by observations of several CAO cases and using LES, we successfully set up and evaluate the evolution of cloud micro- and macrophysical properties
- ▶ The choice of reanalysis dataset for initial and boundary conditions affects simulations
- ▶ As demonstrated here, simulations lack early drizzle and rain that may crucially affect the timing of cloud breakup, further exasperated by a simplified ice treatment

4. EVALUATION (PRELIMINARY)

- ▶ Representative of several CAO cases (Table 1), we examine 18 January 2022
 - This case has uniquely consistent cloud-top heights across observations and simulations when using reanalysis boundary conditions.
 - Translated into fetch, ΔL , using observed cloud edge and reanalysis horizontal wind
- ▶ Meteorological initial and boundary conditions modify the simulated state (Fig. 3) and also impact cloud morphology and cloud transition timing (not shown)
- ERA5 leads to greater turbulent surface fluxes (in line with earlier findings^[9]) producing a swifter cloud buildup (Fig. 3d) in a deeper boundary layer (Fig. 3a), earlier rain onset (Fig. 3g), and transition to the broken state (Fig. 3b), generally matching the observed state better

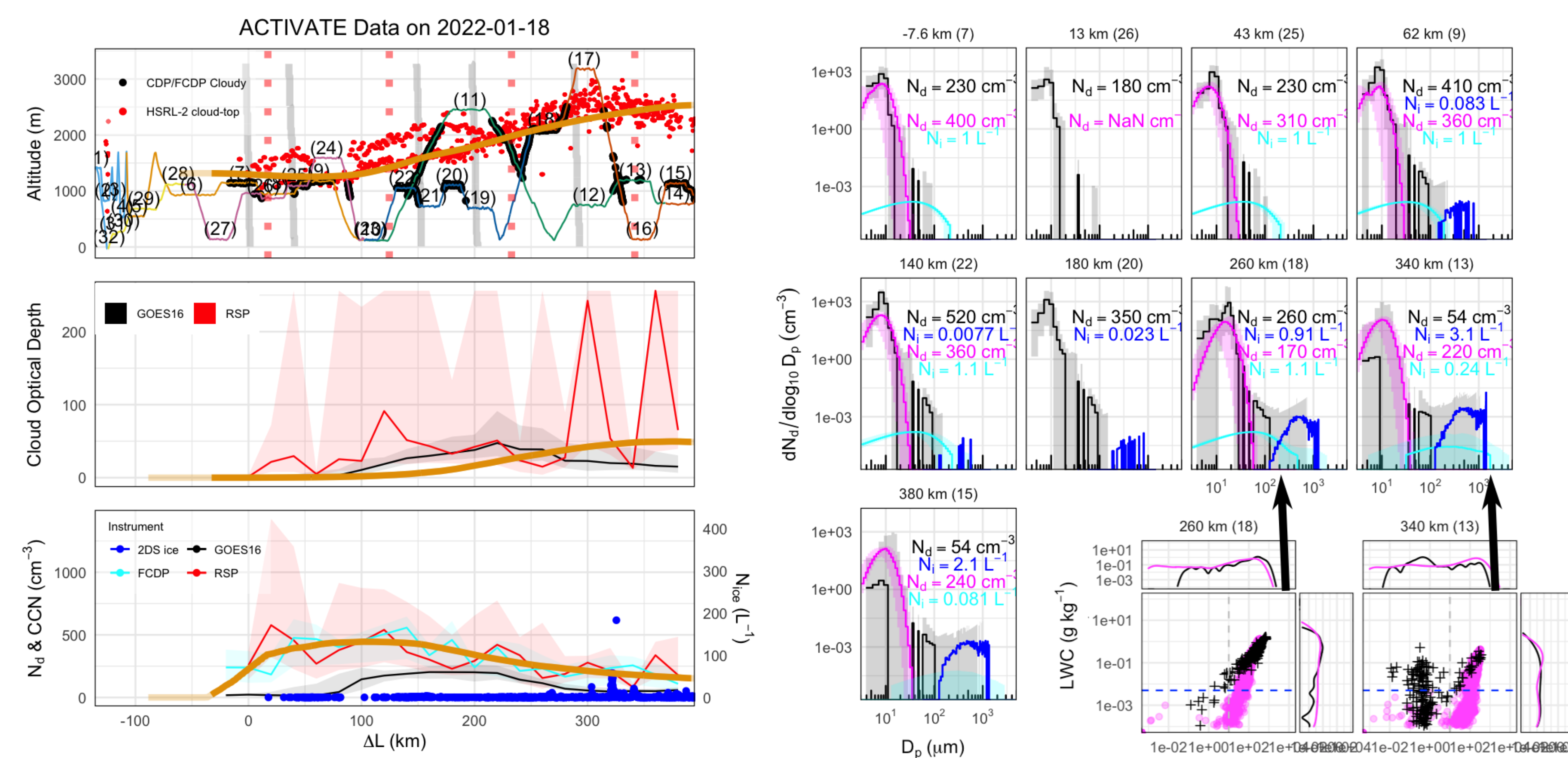


Fig. 4: Evaluating ACTIVATE observations and LES in a quasi-Lagrangian framework. Top left: in-situ flight track and HSRL-2-sensed cloud-top height (red) overlaid with LES inversion height (orange). Middle left: comparing RSP-based and satellite-based cloud optical depth with LES. Bottom left: Comparing N_d retrievals from RSP, FCDP, and GOES16 with LES and also showing 2DS-based N_i . Right: for cloudy legs we compare hydrometeor size distributions of liquid (black for FCDP, magenta for LES) and frozen particles (blue for 2DS, cyan for LES). For two selected panels (indicated through arrows), we also show LWC- N_d scatterplots. The shown simulation uses ERA5 boundary conditions.

4. CONTINUED

- ▶ Comparison of hydrometeor size distributions with fetch (Fig. 4) indicates an earlier and greater drizzle and rain production in obs.
 - Although the N_d evolution is well-matched here by simulations (Fig. 4, bottom left), other cases (not shown) reveal that a lack of early drizzle/rain feeds back with persistence of more droplets in simulations which may delay the cloud transition
- ▶ Greater ice production in the observations results in greater N_i near the transition than upwind (Fig. 4, bottom left)
 - Past work^[6] showed the acceleration of cloud transitions with more ice as a result of riming

3. SETUP OF DHARMA LES^[5,6]

- ▶ Lagrangian domain following PBL horiz. flow
 - $L = 21.6$ km with $dx = 300$ m
 - $H = 5.0$ km with $dz = 40$ m (lowest 3.5 km)
- ▶ Turbulent surface fluxes using similarity theory and fairly modern coefficients^[7]
- ▶ Impose $w_{sub}(z,t)$ and nudging to $\bar{T}(z,t)$ and $\bar{q}_v(z,t)$ in FT and $\bar{u}(z,t)$ and $\bar{v}(z,t)$ above 500m
- ▶ 2-moment cloud (mixed phase) and prognostic 1-moment aerosol microphysics
- ▶ Diagnostic primary ice formation^[8]

#	μ (nm)	σ	κ	N_{PBL} (cm^{-3})	N_{FT} (cm^{-3})
1	10.0	1.70	0.10	0	500
2	32.5	1.35	0.77	50	0
3	118.0	1.54	0.32	500	50

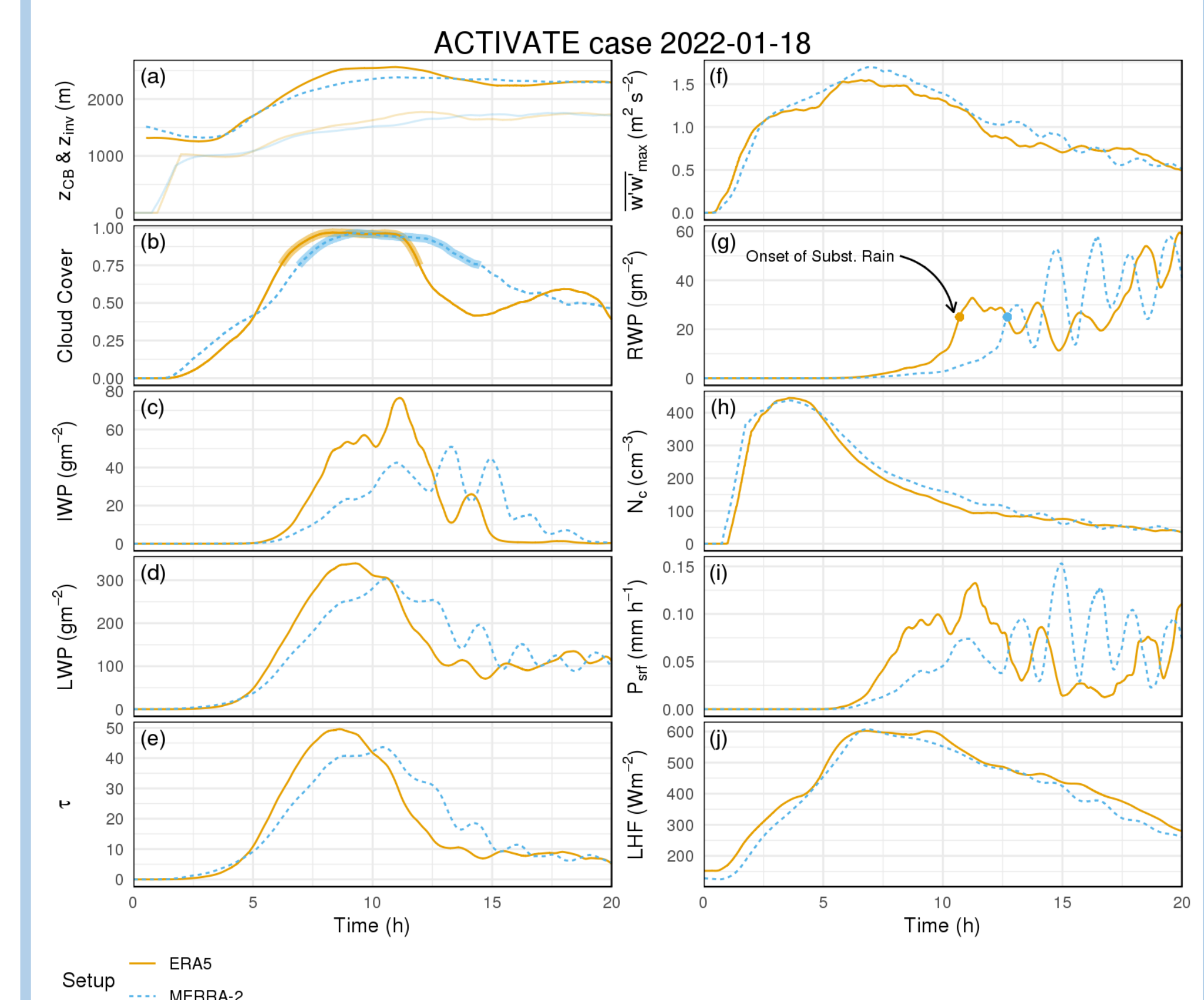


Fig. 3: Large-eddy simulation output from two runs using different meteorological boundary conditions (see legend): (a) cloud-base and inversion height, (b) cloud cover (columns with $COT > 2.5$), (c) ice water path, (d) liquid water path, (e) cloud optical thickness, (f) domain-maximum vertical wind speed variance, (g) rainwater path, (h) cloud droplet number concentration, (i) surface precipitation rate, and (j) surface latent heat flux.

5. OUTLOOK

- ▶ Investigate relative lack of drizzle and rain
 - Use of bin microphysics (that also considers aerosol particles of greater size, Fig. 2)
 - Use of alternative collisional kernels
- ▶ Incorporate observed aerosol hygroscopicity
- ▶ Explore ice formation treatment and ice prop.
- ▶ Run single column version of NASA-GISS ModelE3 with identical forcings

REFERENCES & DATA

- [1] Remilliar and Tselioudis 2015, J. Clim.
- [2] Sorooshian et al. 2019, BAMS
- [3] Tornow et al. 2022, GRL
- [4] Corral et al. 2021, JGR
- [5] Zhou et al. 2017, ACP
- [6] Tornow et al. 2021, ACP
- [7] Zeng et al. 1998, J. Clim.
- [8] Ovchinnikov et al. 2014, JAMES
- [9] Seethala et al. 2021, GRL

Data Available

